A High-affinity Interaction with ADP-Actin Monomers Underlies the Mechanism and In Vivo Function of Srv2/cyclase-associated Protein $\boxed{D}$

Pieta K. Mattila,*[†] Omar Quintero-Monzon,[†‡] Jamie Kugler,[‡] James B. Moseley,[‡] Steven C. Almo,[§] Pekka Lappalainen,* and Bruce L. Goode[‡‖]

*Program in Cellular Biotechnology, Institute of Biotechnology, University of Helsinki, Helsinki 00014, Finland; ‡Department of Biology and The Rosenstiel Basic Medical Science Research Center, Brandeis University, Waltham, MA, 02454; and §Departments of Biochemistry and Anatomy and Structural Biology, and Center for Synchrotron Biosciences, Albert Einstein College of Medicine, Bronx, NY 10461

Cyclase-associated protein (CAP), also called Srv2 in *Saccharomyces cerevisiae*, is a conserved actin monomer-binding protein that promotes cofilin-dependent actin turnover in vitro and in vivo. However, little is known about the mechanism underlying this function. Here, we show that *S. cerevisiae* CAP binds with strong preference to ADP-G-actin (K_d 0.02 μM) compared with ATP-G-actin (K_d 1.9 μM) and competes directly with cofilin for binding ADP-G-actin. Further, CAP blocks actin monomer addition specifically to barbed ends of filaments, in contrast to profilin, which blocks monomer addition to pointed ends of filaments. The actin-binding domain of CAP is more extensive than previously suggested and includes a recently solved β-sheet structure in the C-terminus of CAP and adjacent sequences. Using site-directed mutagenesis, we define evolutionarily conserved residues that mediate binding to ADP-G-actin and demonstrate that these activities are required for CAP function in vivo in directing actin organization and polarized cell growth. Together, our data suggest that in vivo CAP competes with cofilin for binding ADP-actin monomers, allows rapid nucleotide exchange to occur on actin, and then because of its 100-fold weaker binding affinity for ATP-actin compared with ADP-actin, allows other cellular factors such as profilin to take the handoff of ATP-actin and facilitate barbed end assembly.

INTRODUCTION

The actin cytoskeleton plays a critical role in many different cellular processes, including polarity, morphogenesis, motility, endocytosis, and intracellular transport. Various intra- and extracellular signals regulate the structure and dynamics of the actin cytoskeleton through an array of actin-binding proteins. One central family of cytoskeletal regulators is the cyclase-associated proteins (CAPs), which are conserved actin monomer-binding proteins found in all eukaryotes examined so far (reviewed in Hubberstey and Mottillo, 2002). CAP/Srv2 was originally identified in *Saccharomyces cerevisiae* as a protein that interacts with adenylyl cyclase and facilitates its activation by RAS (Fedor-Chaiken *et al.,* 1990; Field *et al.,* 1990). The adenylyl cyclase-binding site is located in the N-terminus of yeast Srv2, but this interaction does not appear to be conserved in animals and plants (Hubberstey and Mottillo, 2002). In contrast, the conserved C-terminal half of this protein is involved in regulating the actin cytoskeleton in all Srv2/CAPs tested so far. The loss of

Srv2 in budding yeast, or deletion of its C-terminus, causes severe defects in the actin cytoskeleton and abnormalities in cell morphology such as cell swelling and a random budding pattern. These phenotypes are partially suppressed by overexpression of the actin monomer-binding protein profilin (Gerst *et al.,* 1991; Vojtek *et al.,* 1991). The loss of Srv2/CAP in *Dictyostelium, Drosophila,* and mammalian cells also results in an accumulation of abnormal actin filament structures and defects in actin-dependent cellular processes such as motility and endocytosis (Baum *et al.,* 2000; Benlali *et al.,* 2000; Noegel *et al.,* 2003; Bertling *et al.,* 2004). In addition, overexpression of Srv2/CAP in plants results in defects in actin filament structures and problems in cell growth and division (Barrero *et al.,* 2002).

Srv2/CAP was originally hypothesized to function as an actin monomer sequestering protein, because it was reported to bind G-actin with 1:1 stoichiometry with a K_d of 0.5–5.0 μM and to suppress the spontaneous polymerization of actin (Gieselmann and Mann, 1992; Freeman *et al.,* 1995; Gottwald *et al.,* 1996; Hubberstey *et al.,* 1996). However, two recent biochemical studies revealed that Srv2/CAPs are not simple actin monomer-sequestering proteins, but instead contribute to actin dynamics by recycling ADF/cofilin and actin monomers for new rounds of actin filament depolymerization and polymerization, respectively (Moriyama and Yahara, 2002; Balcer *et al.,* 2003). These activities are supported by studies in vivo. In yeast, *srv2* mutants display reduced rates of actin patch turnover and have genetic interactions with specific *cof1* alleles (Balcer *et al.,* 2003). In mammalian cells, the depletion of CAP results in an accu-

mulation of ADF/cofilin in abnormal cytoplasmic aggregates and in decreased rates of actin filament depolymerization and polymerization (Bertling *et al.,* 2004).

Although a role for Srv2/CAP in promoting actin dynamics is now clearly demonstrated, the specific nature of the Srv2/CAP-actin monomer interaction underlying this function remains unknown. Many actin monomer-binding proteins, such as profilin, β-thymosins, ciboulot, and MIM (Missing In Metastasis), bind to ATP-G-actin with a higher affinity than ADP-G-actin (Carlier *et al.,* 1993; Vinson *et al.,* 1998; Hertzog *et al.,* 2002; Mattila *et al.,* 2003), whereas ADF/cofilin and twinfilin bind preferentially to ADP-G-actin (Maciver and Weeds, 1994; Carlier *et al.,* 1997; Ojala *et al.,* 2002). The nucleotide preference of actin interactions has important consequences for the roles these proteins play in controlling actin dynamics. Whether Srv2/CAPs prefer ADP- or ATP-G-actin has not been reported. Furthermore, the actin-binding site of Srv2/CAP has not been defined. Based on limited deletion analyses, the actin-binding site was suggested to lie within the C-terminal ~ 150 amino acids of the protein (Gerst *et al.,* 1991; Zelicof *et al.,* 1996). The crystal structure of the C-terminus of Srv2 (residues 369–526) has recently been solved and shown to consist of an unusual β-strand structure that forms a homodimer with an extensive interface (Dodatko *et al.,* 2004). Adjacent to this β-strand domain is a WH2 domain, which is a ubiquitous ATP-G-actin binding protein motif (Baum *et al.,* 2000; Paunola *et al.,* 2002). However, the relative contributions of Srv2/CAP's β-strand and WH2 domains for actin-binding interactions have not been examined.

Here, we report that the C-terminus of yeast Srv2/CAP binds with a strong preference to ADP-actin monomers compared with ATP-actin monomers, competes directly with ADF/cofilin for actin binding, and specifically blocks barbed end assembly. Through deletion analysis, we demonstrate that high-affinity ADP-G-actin binding requires the β-strand region (369–526) and adjacent sequences (253–368) of Srv2. Thus, the actin-binding domain is more extensive than previously suggested. Within the β-strand region, we identified specific surface residues that are critical for high-affinity actin binding. Interestingly, the WH2 domain does not contribute to ADP-actin monomer binding and makes only a minor contribution to ATP-actin interactions. By analyzing these mutants in vivo, we provide direct evidence that ADP-actin monomer binding is essential for the role of Srv2/CAP in regulating actin dynamics and cell morphogenesis in budding yeast.

MATERIALS AND METHODS

Yeast Strains, Cell Growth, and Plasmid Construction

Standard methods were used for all DNA manipulations and for growth and transformation of yeast strains (Rose *et al.,* 1989). Plasmids used in this study are listed in Table 1. A yeast plasmid carrying the wild-type *SRV2* coding sequence under its own promoter was constructed by PCR amplification and subcloning. The coding sequence of wild-type *SRV2* plus 300 bp flanking either side of the open reading frame was PCR amplified from genomic DNA of wild-type yeast (BGY12) using oligonucleotides BG418 and BG419. The PCR insert was subcloned into the *Bam*HI and *Xho*I sites of pRS316 (Sikorski and Hieter, 1989) to make pBG334. To generate specific *srv2* alleles, a PCR-based method of site-directed mutagenesis was used to alter the sequence of the template plasmid pBG334. For each allele, a pair of mutagenic primers was used, indicated in Table 1 which introduce a diagnostic restriction site. The sequences of the oligonucleotides are listed in Table 2.

Plasmids for expressing amino- and carboxyl-terminal fragments of Srv2 protein in *Escherichia coli* were generated by PCR amplifying the appropriate coding sequences from wild-type yeast genomic DNA. The oligonucleotides PL30, PL31, E2369, E2370, and F0254 (listed in Table 2) used in the amplifications generated *Nco*I and *Hin*dIII sites at the 5' and 3' ends of the PCR fragments, respectively. The fragments corresponding to Srv2 amino acids

Table 1. *srv2* mutant alleles generated in this study

Allele	Mutations	Plasmid	Oligonucleotides[a]
SRV2	Wild type	pBG334	—
srv2-101	K325A, K326A	pBG529	BG430, BG431
srv2-102	K367A, R368A	pBG530	BG519, BG520
srv2-103	K378A	pBG531	BG432, BG433
srv2-104	E382A, E385A	pBG532	BG434, BG435
srv2-105	K414A, K416A	pBG533	BG436, BG437
srv2-106	D433A	pBG534	BG438, BG439
srv2-107	D440A	pBG535	BG529, BG530
srv2-108	D461A, K462A	pBG536	BG456, BG457
srv2-109	K472A, E473A	pBG537	BG458, BG459
srv2-110	E495A	pBG538	BG535, BG536
srv2-111	D498A, E501A	pBG539	BG460, BG461
srv2-112	E506A	pBG540	BG539, BG540

[a] Pairs of mutagenic oligonucleotides used to generate *srv2* alleles. Oligonucleotide sequences are listed in Table 2.

1–259, 253–526, and 253–373 were then digested and ligated into the pGAT2 vector (Peränen *et al.,* 1996). Specific mutations were introduced into Srv2$_{253–526}$ and Srv2$_{369–526}$ constructs by site-directed mutagenesis using the pairs of mutagenic oligonucleotides listed in Table 2 and subcloned into *Nco*I-*Hin*dIII digested pGAT2 vector. For expressing the shorter carboxyl terminal fragment of Srv2 (369–526), the DNA encoding these residues was amplified by PCR from wild-type genomic DNA and subcloned into the *Nde*I and *Hin*dIII sites of the pMW172 expression vector (Dodatko *et al.,* 2004).

Protein Expression and Purification

Glutathione-*S*-transferase (GST) fusion proteins of Srv2 fragments and mouse MIM-CT were expressed in *E. coli* BL21 (DE3) cells. The production, thrombin-cleavage, and purification of these proteins was performed as previously described for mouse MIM-CT (Mattila *et al.,* 2003). After separation from GST by thrombin digestion, Srv2$_{253–526}$ was purified further by anion exchange chromatography. Untagged Srv2$_{369–526}$ was purified essentially as described in Dodatko *et al.* (2004). *S. cerevisiae* cofilin, capping protein, and profilin were expressed and purified as described in Amatruda and Cooper (1992), Lappalainen *et al.* (1997), and Wolven *et al.* (2000). Rabbit muscle actin was prepared from acetone powder as described (Pardee and Spudich, 1982).

Actin Monomer-binding Assay

The interaction of wild-type and mutant Srv2 fragments with actin monomers was examined by measuring the fluorescence of NBD-labeled G-actin as described in Mattila *et al.* (2003). Rabbit muscle actin was labeled by NBD-Cl as described in Detmers *et al.* (1981) and Weeds *et al.* (1986). ADP-NBD-actin was prepared by incubation with hexokinase-agarose beads (Sigma, St. Louis, MO) and glucose for 3 h at 4°C (Pollard, 1986). We used 0.2 μM actin and varied the concentration of Srv2 constructs from 0 to 8–20 μM. The reactions were carried out at room temperature in physiological ionic conditions (2 mM Tris, pH 8.0; 0.1 mM CaCl$_2$; 0.1 mM DTT, 0.2 mM ADP or ATP; 0.5 mg/ml bovine serum albumin; 1 mM MgCl$_2$; 0.1 M KCl). The normalized enhancement of fluorescence, as determined by the equation:

$$E = \frac{(F - F0)}{(F\text{max} - F0)}$$

was measured with BioLogic MOS250 fluorometer (Claix, France) at each concentration of Srv2 with an excitation at 482 nm and emission at 535 nm. The data were analyzed using SigmaPlot software and fitted using the following equation:

$$E = \frac{1}{2}c + \frac{1}{2}z - \frac{1}{2}\sqrt{(c + z)^2 - 4z}$$

where z and c are described in the following two equations:

$$z = \frac{[Srv2]tot}{[Act]tot}$$

$$c = 1 + \frac{Kd}{[Act]tot}$$

The competition assays were carried out as described in Ojala *et al.* (2002). The binding was plotted as a function of increasing amounts of Srv2 in the

Table 2. Sequence of oligonucleotides listed 5′ to 3′

Name	Sequence[a]
PL30	CGCGCCATGGCTGACTCTAAGTACACAATGCAAGG
PL31	CGCCAAGCTTAACCAGCATGTTCGAAAACAGCAGA
E2369	GCGCAAGCTTAATTCTTCGTTGATTGTGCCATCG
E2370	CGCGCCATGGCACAATCAACGAAGAATACAGG
F0254	CGCCAAGCTTATTCCTTTCTAGGAGGCCTCTTAG
BG418	CGAATTGGAGCTCCACCGCGGTGGCGGCCGCTCTAGAACTAGTGGATCCTTTACATAAAA
BG419	TTAACCCTCACTAAAGGGAACAAAAGCTGGGTACCGGGCCCCCCCTCGAGATATATGTAT
BG430	GTGAAAATATCACTAAAGGCCTA**GCAGCA**GTAGACAAATCCCAAC
BG431	GTTGGGATTTGTCTAC**TGCTGC**TAGGCCTTTAGTGATATTTTCAC
BG519	CAACATTGAAAACC**GCGGCG**GCCTCCTAGAAAGG
BG520	CCTTTCTAGGAGGC**GCCGCG**GTTTTCAATGTTG
BG432	GAATTGGTAGGAAAC**GCG**TGGTTTATTGAGAATTAC
BG433	GTAATTCTCAATAAACCA**CGC**GTTTCCTACCAATTC
BG434	GAAACAAATGGTTTATC**GCG**AATTACG**CGC**GAATGAAACTGAATCTC
BG435	GAGATTCAGTTTCATT**CGC**GTAATT**CGC**GATAAACCATTTGTTTC
BG436	CAAGTTCTTGTTCAAATA**GCG**GGT**GCC**GTTAACGCTATCTC
BG437	GAGATAGCGTTAAC**GGC**ACC**CGC**TATTTGAACAAGAACTTG
BG438	GCAGTGTTGTTCTT**GCT**AGCAGCATTTCCGGTATG
BG439	CATACCGGAAATGCTGCT**AGC**AAGAACAACACTGC
BG529	GCATTTCCGGGATG**GCA**GTGATCAAATCC
BG530	GGATTTGATCAC**TGC**CATCCCGGAAATGC
BG456	CCTCAAATCTCAATT**GCGGCGT**CTGACGGCGGTAAC
BG457	GTTACCGCCGTCAGA**CGCCGC**AATTGAGATTTGAGG
BG458	GCGGTAACATCTATTTAAGC**GCTGC**TTCCTTGAATACTGAAATC
BG459	GATTTCAGTATTCAAGGA**AGCAGC**GCTTAAATAGATGTTACCGC
BG535	CCAATCGGC**GCC**GACGATGATTACG
BG536	CGTAATCATCGT**CGG**CGCCGATTGG
BG460	CGGCGAGGACGAT**GCA**TATGTAG**GCA**TTCCCAATCCCTG
BG461	CAGGGATTGGGAA**TGC**TACATA**TGC**ATCGTCCTCGCCG
BG539	CCAATCCCT**GCA**CAGATGAAG
BG540	CTTCATCTGT**GCA**CAGGGATTGG

[a] Sequences in bold mark the specific bases that were altered in each *srv2* allele to introduce alanine substitutions.

presence of constant amounts of ATP-actin and MIM-CT, e.g., 0.2 and 0.3 μM, respectively. The data were fitted using the approximated equation:

$$E = \frac{[Srv2]}{K_{Srv2}(1 + [MIM-CT]/K_{MIM-CT}) + [Srv2]}$$

where variable [Srv2] is the concentration of the competing fragment, [MIM-CT] is the constant concentration of MIM-CT, K_{Srv2} and K_{MIM-CT} are the respective dissociation constants (K_{MIM-CT} = 0.06 μM [Mattila *et al.*, 2003]).

Actin Depletion Pull-down Assays

GST-Srv2 fusion proteins were expressed as described for MIM-CT in Mattila *et al.* (2003) in 1–2 liters of Luria broth medium. The cells were resuspended in 30 ml of lysis buffer (10 mM Tris, pH 7.5; 100 mM NaCl; 1 mM DTT; 4 mM EDTA; 0.1% Triton X-100; 0.2 mM PMSF), lysed by sonication, and centrifuged for 60 min at 18,000 $\times$ *g*, and the lysate was passed through a 0.22-μm filter. The fusion proteins were immobilized on glutathione-Sepharose 4B beads (Amersham Pharmacia Biotech, Piscataway, NJ) at a concentration of approximately 5 mg of fusion protein per 2 ml of prewashed beads. The beads were washed twice with 10 ml of lysis buffer and twice with 10 ml of F-buffer (10 mM Tris, pH 7.5; 0.2 mM CaCl$_2$; 0.5 mM DTT; 0.2 mM ADP or ATP, 1 mM MgCl$_2$; 100 mM KCl). The total amount of protein on beads was quantified from a Coomassie-stained SDS-gel of beads. ADP-actin (250 μl of 3 μM) or 2.3 μM ATP-actin was incubated alone or with 9 μM GST or GST-Srv2 fragments coupled to beads for 30 s or 15 min at 25°C. The samples were centrifuged for 5 min at 13,000 $\times$ *g* to pellet the beads and any bound proteins. The amount of actin present in the supernatant was then examined on Coomassie-stained 12% SDS gels. In the cofilin competition assay, GST-Srv2$_{253-526}$ coupled to glutathione-Sepharose 4B beads was preincubated with ADP-actin in a volume of 200 μl. Cofilin was then added to the reaction mix to yield final concentrations of 0, 4.5, 9, 18, 28, and 37 μM cofilin, 3 μM actin, and 9 μM Srv2$_{253-526}$. The reactions were incubated at 20°C for 15 min, and the amount of actin in the supernatants was analyzed as above. The assays were carried out in following buffer conditions: 10 mM Tris, pH 7.5; 0.2 mM CaCl$_2$; 0.5 mM DTT; 0.2 mM ADP or ATP, 1 mM MgCl$_2$; 100 mM KCl.

Actin Filament Elongation Assays

Actin filament elongation assays were performed as described (Moseley *et al.,* 2003). Actin monomers were prepared by gel filtration using a Sephacryl S-200 column equilibrated with G-buffer (10 mM Tris, pH 8.0; 0.2 mM ATP; 0.2 mM CaCl$_2$; 0.2 mM DTT). Actin monomers (40 μl, 0.5 or 3 μM final; 10% pyrene labeled) were preincubated for 2 min with 10 μL HEK buffer (20 mM HEPES, pH 7.5; 1 mM EDTA; 50 mM KCl) or premixed proteins (profilin and/or Srv2) in HEK buffer. Preformed actin filaments (45 μl, 1 μM final) were mixed with 5 μl HEK buffer alone or capping protein in HEK buffer. The actin filaments were sheared by five passages through a 27-gauge needle and syringe. Sheared filaments (20 μl, 333 nM final) were immediately added to actin monomers in F-buffer to initiate elongation. Pyrene fluorescence was monitored at excitation 365 nm and emission 407 nm in a fluorescence spectrophotometer (Photon Technology International, Lawrenceville, NJ). The relative rates of elongation were determined from the slopes of the curves during the early phase of polymerization.

Microscopic Analysis of Yeast Cells

Yeast cells were labeled with rhodamine-conjugated phalloidin after being grown to log phase, fixed for 10 min in 70% ethanol, and processed for fluorescence microscopy (Dewar *et al.,* 2002). Fluorescence images were acquired from a Zeiss E600 microscope (Thornwood, NY) equipped with Hammamatsu Orca ER CCD camera (Bridgewater, NJ) running Open Lab software (Improvision, Lexington, MA).

CD Spectroscopy

CD measurements were recorded with a Jasco J-700 spectropolarimeter equipped with a microcomputer and a Jasco PTC-348WI thermostat. Spectra were collected with a scan speed of 20 nm/min, step resolution of 0.1 nm, bandwidth of 1.0 nm, sensitivity of 100 millidegrees, and with a response time of 0.25 s. Each spectrum was the average of at least five scans. Far UV CD spectra were recorded at a protein concentration of 4 μM in 5 mM Tris, pH 7.5, and 20 mM UV-free NaCl (Sigma-Aldrich) with a 2-mm pathlength optical cell.
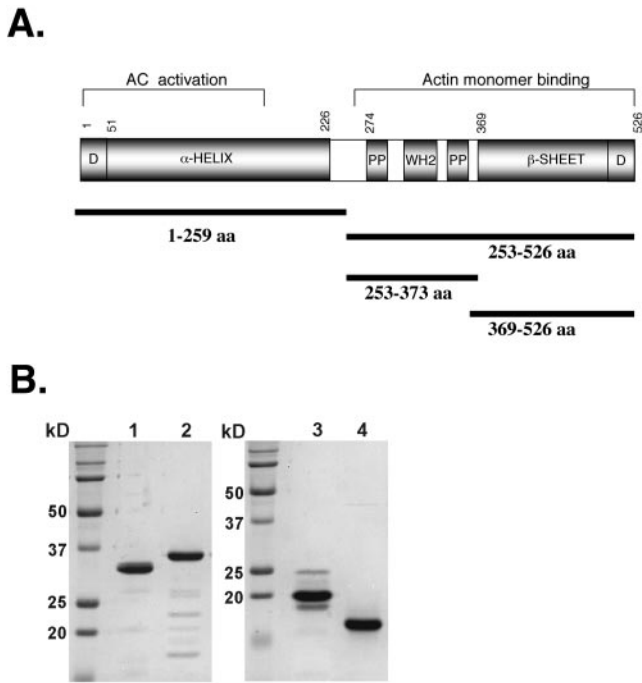
A.

B.

Figure 1. Purified fragments of Srv2/CAP. (A) A schematic representation of Srv2/CAP domains: AC, adenylyl cyclase binding domain; PP, proline-rich motifs (for exact sequences, see Figure 5); WH2, WASp-homology domain 2; D, sites that mediate Srv2/CAP dimerization or multimerization (Huberstey *et al.*, 1996; Zelicof *et al.*, 1996; Yu *et al.*, 1999). The second proline-rich domain binds to the SH3 domain of Abp1 and is required for proper localization of Srv2 in vivo (Lila and Drubin, 1997). The fragments of Srv2/CAP purified and assayed for actin-binding in this study are indicated below by solid lines. (B) Coomassie-stained SDS gel showing the purified Srv2/CAP fragments: lane 1, $Srv2_{1-259}$; lane 2, $Srv2_{253-526}$; lane 3, $Srv2_{369-526}$; and lane 4, $Srv2_{253-373}$.

Miscellaneous

Protein concentrations were determined with a Hewlett Packard 8452A diode array spectrophotometer (Palo Alto, CA) by using the calculated extinction coefficients for *S. cerevisiae* $Srv2_{253-526}$ and $Srv2_{369-526}$ constructs ($\epsilon_{280} = 10,810$ M^{-1} cm^{-1}) and for actin ($\epsilon_{290-320} = 26,600$ M^{-1} cm^{-1}). Where noted (e.g., glutathione beads in pull-down assays), protein concentrations were estimated from Coomassie-stained SDS gels. Fluorescence-monitored urea denaturation assays were performed as described (Lappalainen *et al.*, 1997).

RESULTS

Srv2 Binds with High Affinity and Preference to ADP-G-Actin

Actin-binding proteins regulate many different steps of actin assembly and turnover. One central property of proteins that can help define their precise role in controlling actin dynamics is their preference for binding ADP- or ATP-actin. To compare the interactions of yeast Srv2 with ADP-G-actin and ATP-G-actin, we expressed its C-terminal half ($Srv2_{253-526}$) in *E. coli* as a GST-fusion protein (Figure 1B, lane 2). This C-terminal fragment of Srv2/CAP has been reported to harbor the full actin monomer-binding activity of these proteins (Moriyama and Yahara, 2002).

The fluorescence of NBD-labeled actin monomers is affected by interaction with many actin-binding proteins, including ADF/cofilin, twinfilin, thymosin-β4, and MIM (Missing In Metastasis), thereby providing a method to determine the affinities of these proteins for actin monomers
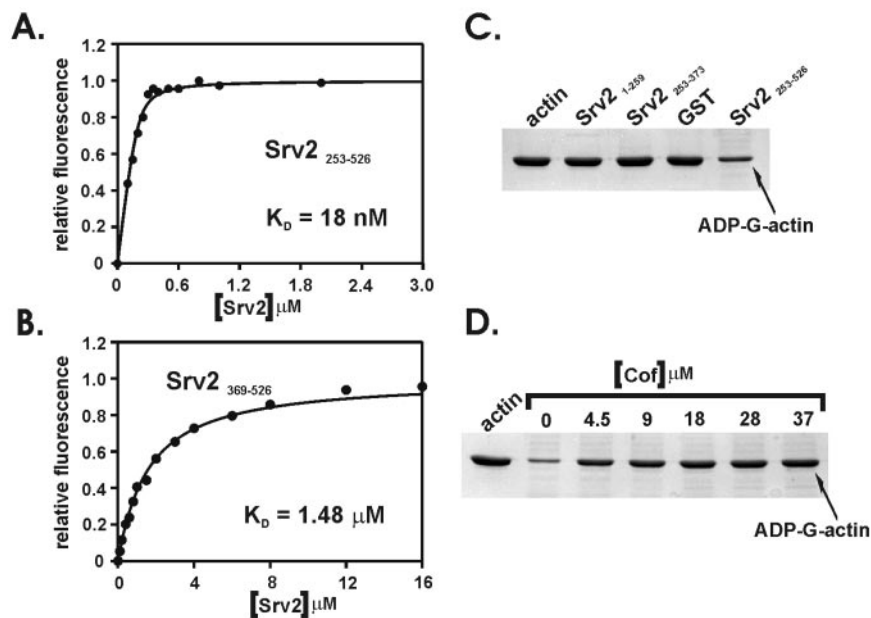
(Carlier *et al.*, 1997; Hertzog *et al.*, 2002; Ojala *et al.*, 2002; Mattila *et al.*, 2003). $Srv2_{253-526}$ induced approximately a 35% increase in the fluorescence of ADP-NBD-G-actin. The extent of the NBD-actin fluorescence increase displayed a saturating behavior, enabling us to calculate the K_d values for Srv2-ADP-actin monomer complexes. These data show that $Srv2_{253-526}$ binds ADP-actin monomers with very high affinity ($K_d = 0.018$ μM; Figure 2A).

In contrast, addition of $Srv2_{253-526}$ to ATP-actin monomers did not affect NBD-actin fluorescence, suggesting that $Srv2_{253-526}$ either does not bind ATP-actin with a detectable affinity or that the binding to ATP-actin monomers does not induce a change in the NBD-fluorescence. We thus carried out a competition assay to examine the affinity of $Srv2_{253-526}$ for ATP-actin. In these experiments we examined the ability of $Srv2_{253-526}$ to displace another actin monomer binding protein, MIM (Missing In Metastasis), from actin monomers. The C-terminal half of mouse MIM binds ATP-G-actin with high affinity ($K_d = 0.06$ μM) and when bound induces a 20–25% quenching of the NBD-actin fluorescence (Mattila *et al.*, 2003). Addition of $Srv2_{253-526}$ to MIM-CT/ATP-G-actin complexes resulted in an increase in the fluorescence. This fluorescence increase showed saturating behavior, which enabled us to calculate the affinity of $Srv2_{253-526}$ for ATP-G-actin ($K_d = 1.9$ μM; Figure 3A). The assays were carried out under physiological ionic conditions (100 mM KCl, pH 8.0).

The preference of Srv2 for ADP-G-actin over ATP-G-actin was confirmed by using an actin depletion pull-down assay. These assays were carried out with 2.3 or 3 μM ATP- or ADP-actin monomers, respectively. Because a significant proportion of ATP-actin is expected to polymerize under physiological ionic conditions after prolonged incubation, the assay was carried out using both 30-s and 15-min incubation times after the addition of monomeric actin and salt on Srv2-glutathione beads. In both cases the results were essentially the same, indicating that actin polymerization does not have a significant effect on the results of this assay. $GST-Srv2_{253-526}$ coupled to the glutathione-Sepharose beads efficiently depleted ADP-actin from the supernatant fraction, whereas it did not have detectable effect on the level of ATP-actin in the supernatant (Figure 3B). Together with fluorometric NBD-actin assays, these data show that Srv2 binds ADP-G-actin with very high affinity, whereas it interacts with ATP-G-actin with only a modest affinity. Consistent with previous reports using intact CAP (Moriyama and Yahara, 2002; Balcer *et al.*, 2003), we found that $Srv2_{253-526}$ had unappreciable affinity for F-actin in cosedimentation assays (Supplementary Figure S1).

Srv2 Directly Competes with Cofilin for Binding to Actin Monomers

Srv2/CAPs promote actin dynamics by recycling ADF/cofilin for new rounds of actin filament depolymerization and recycling G-actin for new rounds of polymerization (Moriyama and Yahara, 2002; Balcer *et al.*, 2003; Bertling *et al.*, 2004). To understand the mechanism by which Srv2 recycles ADF/cofilin, it was important to test whether these two actin monomer-binding proteins compete with each other in binding to ADP-G-actin. Because both yeast Srv2 and cofilin induce a similar increase in the fluorescence of NBD-actin monomers, the possible Srv2/cofilin competition for actin binding could not be examined by an assay similar to the one described above for Srv2 and MIM proteins. Therefore we used an actin depletion pull-down assay for this purpose. $GST-Srv2_{253-526}$–coupled glutathione-Sepharose beads were incubated with ADP-actin monomers and variable concentrations of yeast cofilin. The beads were sedi-

Figure 2. Srv2$_{253-526}$ binds ADP-actin monomers with high affinity and competes with cofilin for binding actin. (A and B) The increase in the fluorescence of 0.2 μM NBD-labeled MgADP-G-actin was measured under physiological ionic conditions at pH 8.0 over a range of concentrations of Srv2$_{253-526}$ (A) and Srv2$_{369-526}$ (B). Symbols are data, and lines are the calculated binding curves for a complex with 1:1 stoichiometry. Dissociation constants (K_d) were calculated from the binding curves in the figures as described in *Materials and Methods*. (C) Srv2$_{253-526}$ depletes significant amounts of ADP-actin from the supernatant in a pull-down assay, whereas Srv2$_{253-373}$ and Srv2$_{1-259}$ fragments or GST alone do not. The concentrations of actin and GST-fusion proteins in this assay were 3 and 9 μM, respectively. The leftmost lane shows the amount of actin in the supernatant when the control assay was carried out without glutathione beads. (D) Yeast cofilin and Srv2$_{253-526}$ compete with each other in actin binding. The ADP-actin concentration in the supernatant depletion pull-down assay wa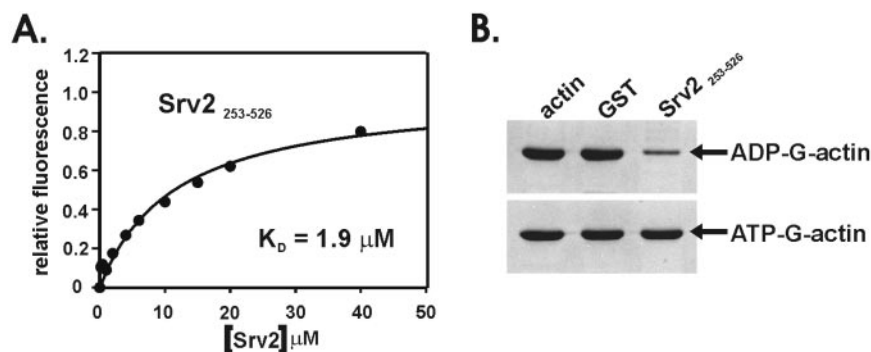s 3 μM, and the concentration of GST-Srv2$_{253-526}$ was 9 μM. Addition of soluble yeast cofilin (4.5–37 μM) decreases the amount of actin monomers sequestered by GST-Srv2$_{253-526}$. The leftmost lane shows the amount of actin in the supernatant when the assay was carried out in the absence of cofilin and GST-Srv2$_{253-526}$.

mented by centrifugation and the amount of actin left in the supernatant was quantified on an SDS gel. In the absence of cofilin, GST-Srv2$_{253-526}$ efficiently decreased the amount of ADP-G-actin in the supernatant. However, addition of soluble cofilin to the reactions decreased the amount of actin monomers sequestered by GST-Srv2$_{253-526}$ (Figure 2D). These data show that yeast cofilin and Srv2 directly compete with each other for binding to actin monomers.

Srv2 Blocks the Addition of Actin Monomers to Filament Barbed Ends

Actin monomer-binding proteins interact with G-actin in distinct ways and can thereby block monomer addition specifically at pointed ends of filaments (e.g., profilin), barbed ends of filaments (e.g., DNAse I), or both ends (e.g., thymosins and twinfilins). To better characterize the Srv2-G-actin interaction, we measured rates of addition of Srv2$_{253-526}$-bound actin monomers to barbed and pointed ends of preformed actin filaments (Figure 4). Sheered actin filaments were used, and the concentration of ends was constant in these reactions. In the presence of 3 μM monomers, a concentration well above the pointed and barbed end critical

concentrations (Pollard, 1986), elongation occurs at both ends of filaments. Addition of *S. cerevisiae* profilin to these reactions decreased the rate of elongation modestly, by 15–20%, consistent with profilin restricting elongation to the faster-growing barbed ends. In contrast, addition of *S. cerevisiae* capping protein decreased the rate of elongation by 80–85%, consistent with capping barbed ends and restricting elongation to the slower-growing pointed ends. Addition of Srv2$_{253-526}$ decreased the rate of elongation 80–85% (Figure 4, A and B), suggesting that Srv2$_{253-526}$ inhibits barbed end growth but allows pointed end growth. Testing a range of Srv2$_{253-526}$ and capping protein concentrations showed that their effects both saturate at 80–85% inhibition.

To test more directly the effects of profilin, capping protein, and Srv2 specifically on barbed end growth, we measured filament elongation in the presence of 0.5 μM actin monomers. These conditions restrict growth to the barbed end, because the actin monomer concentration is below the pointed end critical concentration (Moseley *et al.*, 2003). As expected, profilin had no effect on rate of elongation and capping protein abolished all elongation (Figure 4, C and D). Srv2$_{253-526}$ abolished all elongation, indicating that Srv2

Figure 3. Srv2$_{253-526}$ binds ATP-actin monomers with only a modest affinity. (A) Competition for ATP-actin binding between MIM-CT and Srv2$_{253-526}$. A range of Srv2$_{253-526}$ concentrations were added to reactions containing 0.2 μM ATP-actin and 0.3 μM MIM-CT at PH 8.0, and the change in fluorescence was measured. Symbols are data, and the solid lines are fitted binding curves for a complex with 1:1 stoichiometry. (B) Determination of the actin nucleotide state binding preference of Srv2$_{253-526}$ by actin depletion pull-down assay. Reactions contained 3 μM ADP-actin, 2.3 μM ATP-actin, and 9 μM GST-Srv2$_{253-526}$. As controls, the levels of actin in the supernatants are shown for reactions containing GST alone or lacking glutathione-agarose beads.

blocks monomer addition to barbed ends. A similar inhibitory activity was observed using the shorter Srv2$_{369-526}$ fragment (Figure 4E), but required higher Srv2 concentrations than with Srv2$_{253-526}$, consistent with the weaker affinity of this construct for G-actin. We then tested the ability of profilin to relieve inhibition of barbed end addition by Srv2$_{253-526}$. In reactions containing filament seeds, 10 μM Srv2$_{253-526}$, and either 0.5 μM or 3 μM actin monomers, addition of 10–30 μM profilin increased the rate of elongation (Figure 4, A–D). Thus, Srv2$_{253-526}$ inhibits monomer addition at barbed ends, and profilin can partially relieve this inhibition, suggesting a handoff of ATP-actin monomers from Srv2 to profilin.

Identification of the Actin-binding Site on Srv2

To map the actin-binding site on Srv2, we first compared the affinities of Srv2$_{253-526}$ construct and a shorter "β-strand domain construct, " Srv2$_{369-526}$ (Figure 1A), for ADP-G-actin. This shorter construct includes the last 160 residues of Srv2, which previous deletion studies suggested contain the full actin-binding affinity of Srv2 (reviewed in Hubberstey and Mottillo, 2002). Srv2$_{369-526}$ induced a 50–75% increase in the fluorescence of NBD-ADP-actin, from which we could calculate its affinity for actin monomers. Interestingly, these data revealed that the shorter Srv2$_{369-526}$ fragment has ~75-fold weaker affinity for ADP-G-actin (K_d = 1.48 μM) compared with the longer construct Srv2$_{253-526}$ (K_d = 0.018 μM; Figure 2, A and B). It is important to note that Srv2(253–526) and Srv2(369–526) fragments show overall stability similar to each other. In the fluorescence-monitored urea denaturation assay, the behavior of both fragments was consistent with a simple two-state unfolding transition and both fragments showed a midpoint for the transition at approximately 4 M urea (see Figure 9).

To assess the possibility that there might be two independent actin-binding sites in Srv2, we tested whether the N-terminal half of this protein, Srv2$_{1-259}$, or the fragment containing the proline-rich regions and WH2 domain, Srv2$_{253-373}$, could bind actin (schematic and purified proteins in Figure 1). Neither of these fragments provided detectable signal with ADP-actin in an NBD assay, suggesting that either they do not bind actin or that the binding does not induce a signal in NBD fluorescence. To distinguish between these two alternatives, we next carried out a supernatant depletion pull-down assay. GST-Srv2$_{1-259}$ and GST-Srv2$_{253-373}$ coupled to the glutathione-Sepharose beads were unable to bind detectable amounts of ADP-G-actin, while Srv2$_{253-526}$ efficiently depleted actin from the supernatant (Figure 2C).

Identification of Residues in the C-terminal Region of Srv2 Required for Function In Vivo

To identify residues in the C-terminus of Srv2 that mediate actin binding, we generated 12 mutant alleles, each with 1–2 charge-to-alanine substitutions at evolutionarily conserved, solvent-exposed residues (see alignment in Figure 5 and Table 1). The mutations in 10 alleles (srv2-103 to srv2-112) can be modeled on the recently solved crystal structure of Srv2$_{369-526}$ (Figure 6). The structure is a tightly interlaced homo-dimer with each half comprised of β-sheets and connecting loops arranged into a helix. Mutations in four alleles reside on surfaces of the β-sheets (Figure 2, srv2-103, srv2-104, srv2-107, and srv2-111), whereas mutations in six other alleles reside in connecting loops (srv2-105, srv2-106, srv2-108, srv2-109, srv2-110, and srv2-112). Two additional alleles (srv2-101 and srv2-102) introduce mutations N-terminal to Srv2$_{369-526}$ and thus are not shown in Figure 6. srv2-101 is of

particular interest, because it introduces alanine substitutions at highly conserved residues in the WH2 domain, and the same mutation disrupts interactions with ATP-G-actin in other WH2 domains (Van Troys et al., 1996; Vaduva et al., 1999; Yamaguchi et al., 2000; Mattila et al., 2003; Hertzog et al., 2004).

We analyzed the srv2 allele collection for defects in vivo similar to those caused by srv2Δ null mutants or truncations of the Srv2 C-terminus. These phenotypes include 1) severe depolarization of cortical actin patches and reduction of actin cable staining, 2) impaired growth at 37°C, and 3) a prevalence of enlarged and rounded mother cells and some multibudded cells (i.e., indicative of cell polarity defects). For these analyses, an srv2 null yeast strain was transformed with low copy plasmids carrying wild-type or mutant alleles of the SRV2 gene, expressed under the control of its own promoter. Cells were compared for growth at 25 and 37°C (Figure 7). The srv2 null cells grow poorly at 37°C, but are rescued by the wild-type SRV2 plasmid, and 9 of the 12 srv2 alleles rescued growth at 37°C similar to wild-type SRV2. These alleles caused no detectable phenotypes in actin organization or cell morphology (unpublished data). In contrast, the remaining three srv2 alleles (srv2-104, srv2-108, and srv2-109) each failed to rescue cell growth of the srv2 null strain at 37°C (Figure 7) and showed dramatic defects in actin organization and cell morphology (Figure 8). In each of these mutants, polarization of the actin cytoskeleton was severely disrupted, similar to the srv2 null mutation, but there were noticeable differences in the cellular morphologies. srv2-104 closely resembled the srv2Δ cell morphology, with enlarged mother cells, small daughter cells, and a frequent occurrence of multibudded cells (~5–10% of cells). srv2-108 and srv2-109 mother cells also were enlarged, but had a high abundance of daughter cells with elongated buds, and the multibudded phenotype was much less frequent.

Residues Required for Srv2/CAP Function In Vivo Mediate Actin Binding In Vitro

Next, we sought to determine whether the in vivo defects observed above for specific srv2 alleles might be caused by defects in actin binding. To address this, we analyzed the ADP-G-actin binding affinities of select srv2 alleles introduced into the Srv2$_{253-526}$ fragment. Three alleles (Srv2-104, Srv2-108, and Srv2-109) were chosen because they cause severe defects in actin organization and temperature sensitive growth (Figures 7 and 8). A fourth mutant, srv2-101, was selected because the residues mutated (Lys325 and Lys326) reside in the WH2 domain and are critical for G-actin binding in other WH2 domains such as thymosin-β4 (Van Troys et al., 1996). To compare the stability and structure of the purified Srv2$_{253-526}$ and Srv2-104$_{253-526}$, Srv2-108$_{253-526}$, and Srv2-109$_{253-526}$ proteins, we carried out a fluorescence-monitored urea denaturation assay and measured the far UV CD spectra (Figure 9). The urea denaturation assay showed that the mutants unfolded at a slightly lower urea concentration (2.8–3.5 M) than the wild-type protein (4 M). However, the far UV CD spectra were nearly identical, indicating that the compositions of secondary structure elements in these proteins are very similar.

The purified mutant Srv2$_{253-526}$ proteins, Srv2-104, Srv2-108, and Srv2-109, each showed reduced affinity for ADP-G-actin (3.5–7-fold) compared with wild-type protein (Figure 10A). However, the Srv2-101$_{253-526}$ construct, in which the WH2 domain was inactivated, bound ADP-G-actin with an affinity similar to the wild-type Srv2$_{253-526}$. We also selected one of these mutants, Srv2-104, to examine its effect to
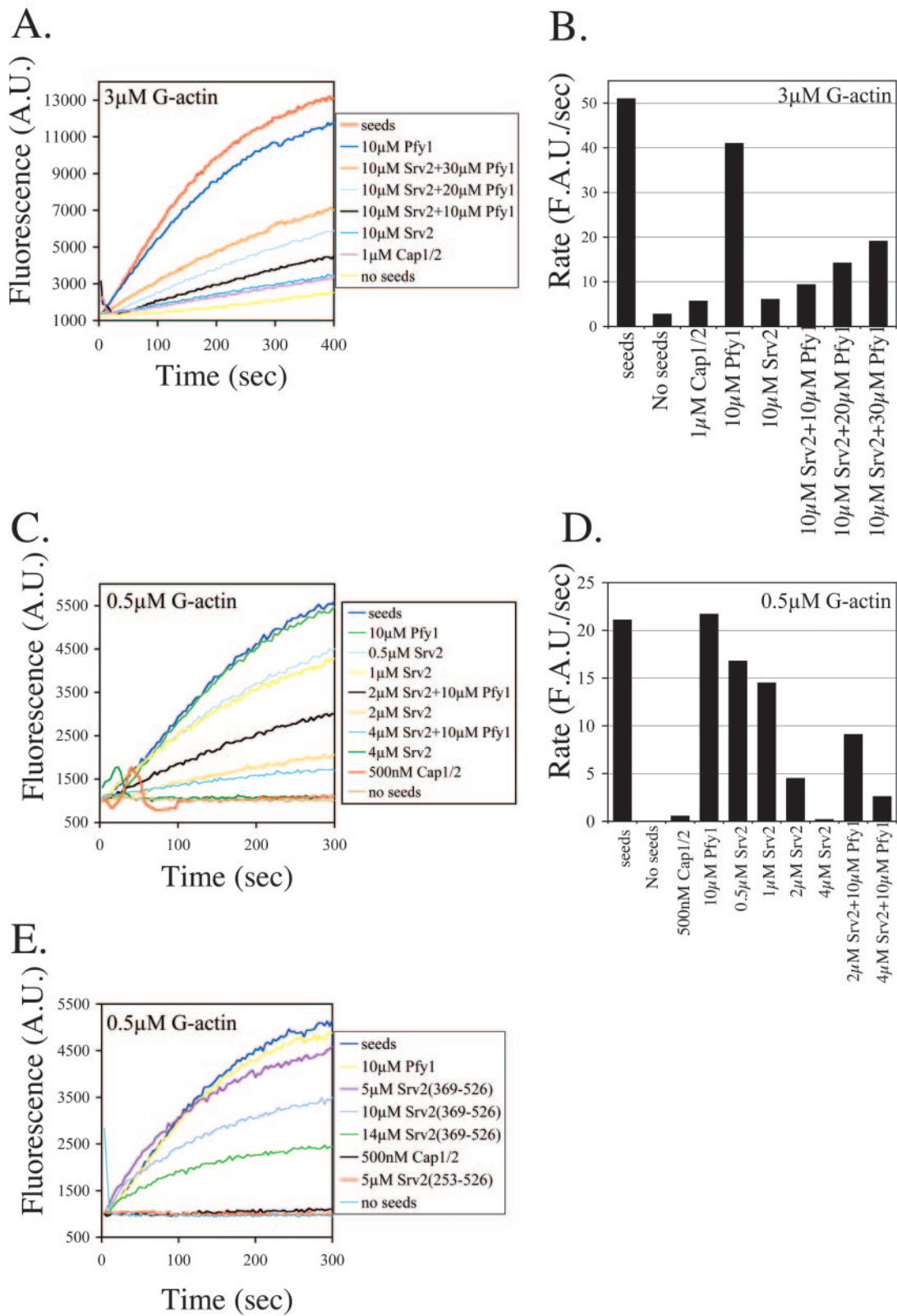
Figure 4. Srv2 inhibits actin monomer addition to barbed ends of filaments. (A) Monomeric actin (3 μM; 10% pyrene-labeled) was preincubated with profilin and/or Srv2$_{253–526}$ (final concentrations indicated) and added to mechanically sheared actin filament seeds (333 nM) to assay elongation at barbed and pointed ends. (B) Rates of filament elongation from A were calculated as in Moseley *et al.* (2003). (C) Monomeric actin (0.5 μM; 10% pyrene-labeled) was preincubated with profilin and/or Srv2$_{253–526}$ and added to F-actin seeds as in A to initiate elongation specifically at the barbed ends of filaments. (D) Rates of filament elongation from C. (E) The same as C, but testing effects of Srv2$_{369–526}$ on elongation at barbed ends of filaments.
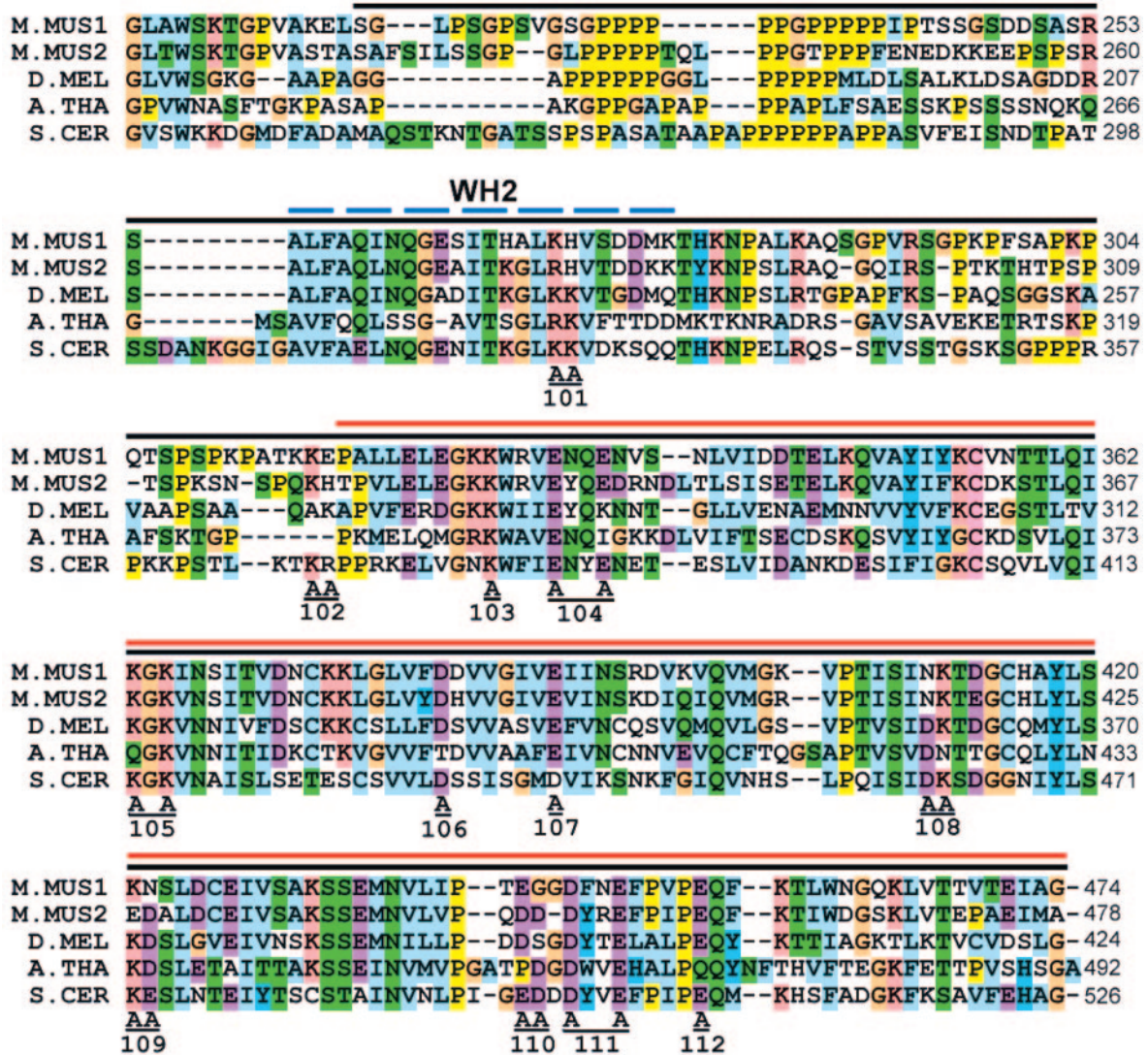
Figure 5. Alignment of CAP sequences from multiple species. Amino acid sequences from the C-terminal halves of mouse CAP1 and CAP2, *Drosophila melanogaster* CAP, *Arabidopsis thaliana* CAP, and *S. cerevisiae* Srv2/CAP were aligned using the Clustal X program. Regions encompassed by the Srv2$_{253-526}$ and Srv2$_{369-526}$ constructs are indicated by lines above the alignment, and the position of WH2 domain is indicated by a dashed line. The residues replaced by alanine in each *srv2* allele (101–112) generated in this study (see Table 1) are indicated below the aligned sequences.

ADP-G-actin binding in the context of the shorter actin-binding construct, Srv2-104$_{369-526}$. This mutation caused >2-fold decrease in the affinity for ADP-G-actin, confirming that these residues are important for actin binding in Srv2 (Figure 10B). These data are summarized in Table 3.

Although Srv2 binds to ATP-G-actin only with a modest affinity, we also tested the effects of two selected mutants (Srv2-101 and Srv2-104) for ATP-G-actin binding. The data from a competition binding assay with MIM showed that Srv2-104$_{253-526}$ binds ATP-G-actin with an affinity very similar to wild-type Srv2$_{253-526}$, whereas Srv2-101$_{253-526}$ shows slightly reduced affinity for ATP-G-actin (Figure 10C). These data indicate that, although the WH2 domain does not contribute to ADP-G-actin binding in Srv2, it is involved to some degree in ATP-G-actin binding. The data show that different regions of Srv2 can be involved in binding ATP- and ADP-actin.

Finally, we addressed the possible effects of these mutations on formation of the Srv2/CAP high-molecular-weight (HMW) complex. Native Srv2/CAP exists in a 15–16S complex in cell extracts, and purified Srv2/CAP oligomerizes via interactions within and between its N- and C-termini (Hubberstey *et al.*, 1996; Zelicof *et al.*, 1996; Yu *et al.*, 1999; Balcer *et al.*, 2003). Because assembly into a HMW complex may be an important requirement for Srv2/CAP function in vivo, we considered the possibility that some of the point mutations with strong phenotypes might interfere with N- and C-terminal interactions and thereby destabilize the complex. To test this, we compared the migration of Srv2 in cell extracts from wild-type, *srv2-108*, and *srv2-109* strains fractionated by sedimentation velocity on sucrose gradients (by immunoblotting fractions for Srv2). However, no differences in migration of the wild-type and mutant Srv2 complexes were observed (Quintero-Monzon and Goode, unpub-

Table 3. Biochemical properties of purified Srv2 fragments

Srv2 fragment	Affinity for actin monomers K_d (μM)[a]	
	ADP-actin	ATP-actin
Srv2$_{253-526}$	0.02	1.9
Srv2-101$_{253-526}$	0.02	3.3
Srv2-104$_{253-526}$	0.07	1.9
Srv2-108$_{253-526}$	0.14	n.d.[b]
Srv2-109$_{253-526}$	0.12	n.d.
Srv2$_{369-526}$	1.5	n.d.
Srv2-104$_{369-526}$	3.2	n.d.
Srv2$_{253-373}$	No[c]	n.d.
Srv2$_{1-259}$	No[c]	n.d.

[a] Determined by NBD-actin binding assays (see *Materials and Methods*).

[b] n.d., not detected.

[c] No NBD-actin signal and no binding detected in GST pull-down assays (see *Materials and Methods*).

lished data). Therefore, the mutations *srv2-108* and *srv2-109* primarily affect actin binding, and HMW complex formation is not grossly impaired. These data show that formation of the HMW complex does not require high-affinity actin binding, which agrees with observation that purified full-length CAP oligomerizes as a hexamer in the absence of actin (Ksiazek *et al.*, 2003).

DISCUSSION

Srv2/CAP is one of the most widely conserved actin-binding protein families found in eukaryotic cells, yet until recently its cellular function was not well understood. Early work suggested that Srv2/CAP might be an actin monomer sequestering protein, but recent studies demonstrate that it has a more active and complex role in controlling actin filament dynamics. Srv2/CAP assembles into an HMW complex (~600 kDa), estimated to be comprised of six Srv2 and six actin molecules (Balcer *et al.*, 2003), and interacts with at least three other actin-binding proteins, Abp1 (Free-
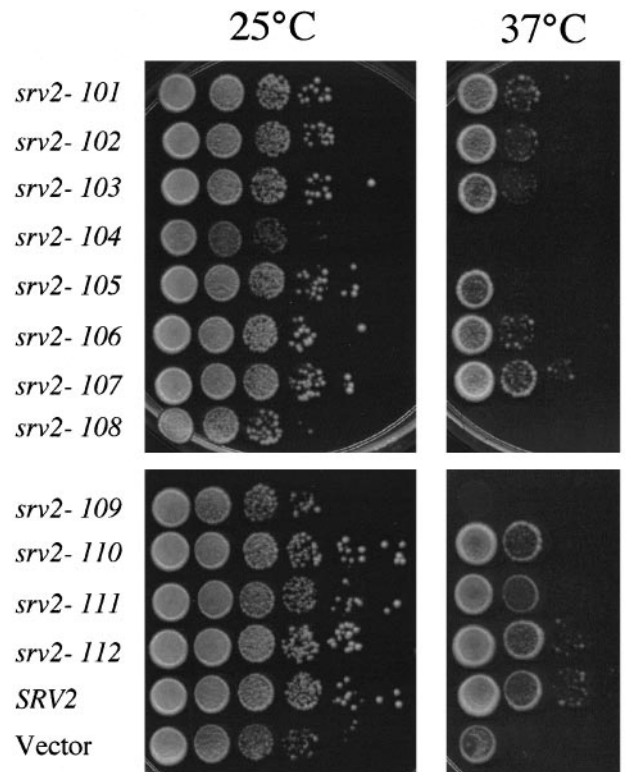

Figure 7. Growth phenotypes of yeast cells expressing wild-type and mutant alleles of the *SRV2* gene. An *srv2* null strain of *S. cerevisiae* (BGY330) was transformed with low copy plasmids expressing wild-type or mutant *srv2* alleles under the control of the *SRV2* promoter. Transformed cells were grown to saturation, plated in 10-fold serial dilutions, and grown at 25 or 37°C.

man *et al.*, 1996; Lila and Drubin, 1997; Balcer *et al.*, 2003), cofilin (Moriyama and Yahara, 2002), and profilin (Drees *et al.*, 2000). This complex promotes the cofilin-dependent turnover of actin filaments in vitro and in vivo (Moriyama and Yahara, 2002; Balcer *et al.*, 2003; Bertling *et al.*, 2004).
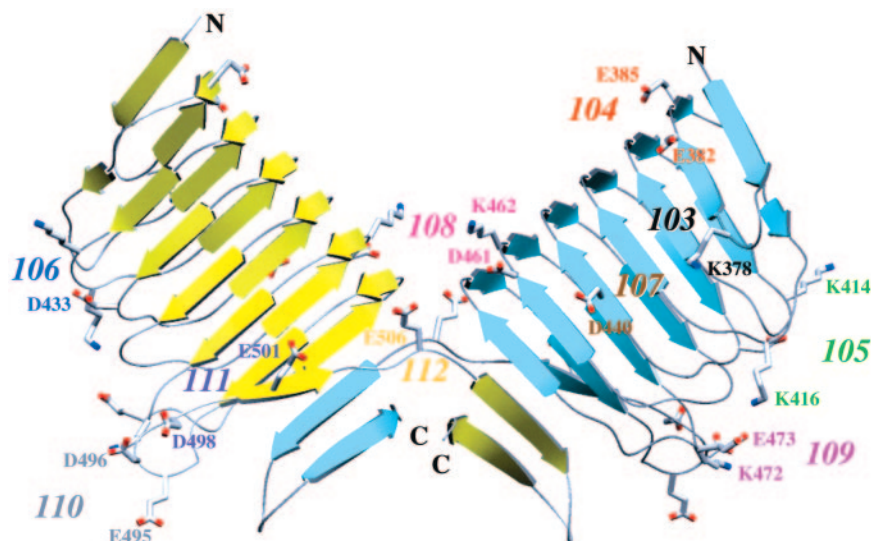

Figure 6. Structural positions of mutated residues in *srv2* alleles. The ribbon structure of the dimeric C-terminus (amino acids 369–526) of *S. cerevisiae* Srv2 is shown (PDB code 1K4Z, details of the structure in Dodatko *et al.*, 2004); the two Srv2 monomers are colored yellow and aqua. Residues altered in each allele are color coded, and each allele is highlighted only once on the two-fold symmetric dimer. Each labeled residue was altered to alanine in the relevant allele (Table 1). Srv2-101 and Srv2-102 are not shown, because the residues altered in these two alleles reside outside of the structurally solved domain.
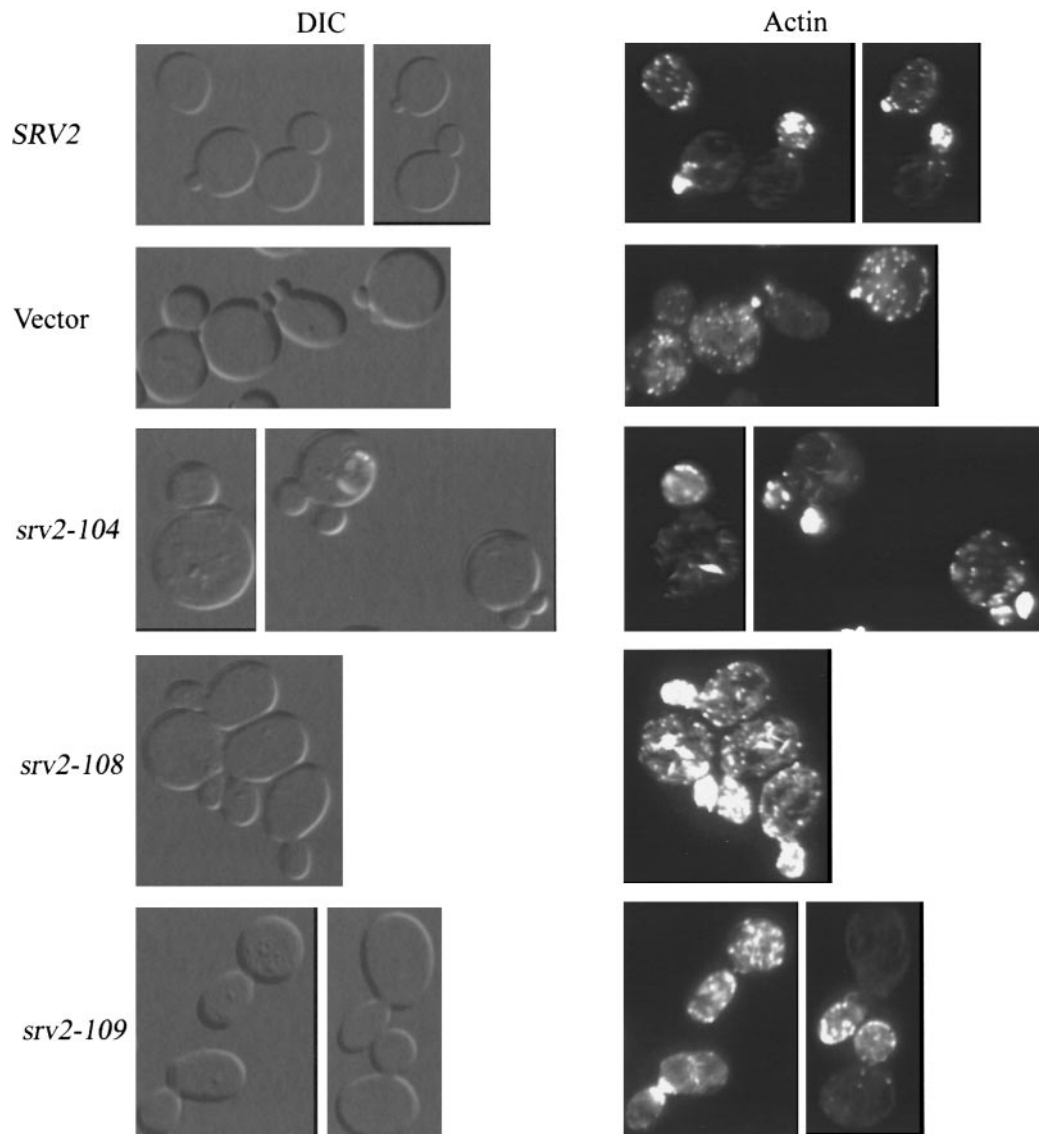
Figure 8. Actin organization defects in cells expressing specific *srv2* mutant alleles. *srv2Δ* cells were transformed with low copy plasmids expressing wild-type *SRV2*, vector alone, or specific *srv2* alleles (*srv2-104*, *srv2-108*, and *srv2-10*) under the control of the *SRV2* promoter. Cells were grown to log phase at 25°C, fixed, and stained with rhodamine phalloidin.

From these studies, it has been suggested that Srv2/CAP promotes recycling of cofilin and actin monomers, thereby accelerating actin filament turnover. However, the mechanism underlying this function has been unclear, in large part because the Srv2/CAP-actin interaction has not been characterized.

Here, we have defined the properties of the yeast Srv2/CAP-actin interaction, providing new insights into how Srv2/CAP proteins promote actin turnover. We show that Srv2/CAP binds with strong preference to ADP-actin monomers compared with ATP-actin monomers and directly competes with cofilin for binding to ADP-actin. This explains how Srv2 can recycle ADP-G-actin from a cofilin-bound state and release monomers after they have undergone nucleotide exchange. Srv2 also blocks ATP-actin monomer addition to barbed ends of filaments, suggesting that in vivo Srv2 acts as a middleman and there is a handoff to other actin monomer binding proteins with a higher affinity for ATP-G-actin such as profilin. Consistent with this idea, we show that profilin partially restores barbed end growth in the presence of Srv2 in vitro. We also find that the actin-binding domain of Srv2 is much more extensive than

previously suggested. The recently solved β-sheet structure $Srv2_{369-526}$ is sufficient to bind actin monomers, but it does so with low affinity, and high-affinity binding requires additional flanking sequences (aa 253–368). Our mutational analyses map actin binding activity in the β-sheet domain to several evolutionarily conserved surfaces. Finally, by analyzing the growth, morphology, and actin organization in cells expressing these mutants, we demonstrate that a strong interaction between Srv2/CAP and ADP-actin monomers is required for Srv2/CAP function in vivo.

The Biochemical Nature of the Srv2-Actin Interaction
Our data show that the boundaries of the Srv2/CAP actin-binding domain extend beyond those previously reported, which were suggested to be contained within the β-sheet region (aa 369–526). This fragment alone has ~75-fold lower ADP-actin binding than a larger C-terminal fragment (aa 253–526) that includes a WH2 domain and other sequences. Nevertheless, within the larger C-terminal fragment (aa 253–526), the β-sheet structure is absolutely critical for actin binding, because the adjacent sequences alone (aa 253–373)
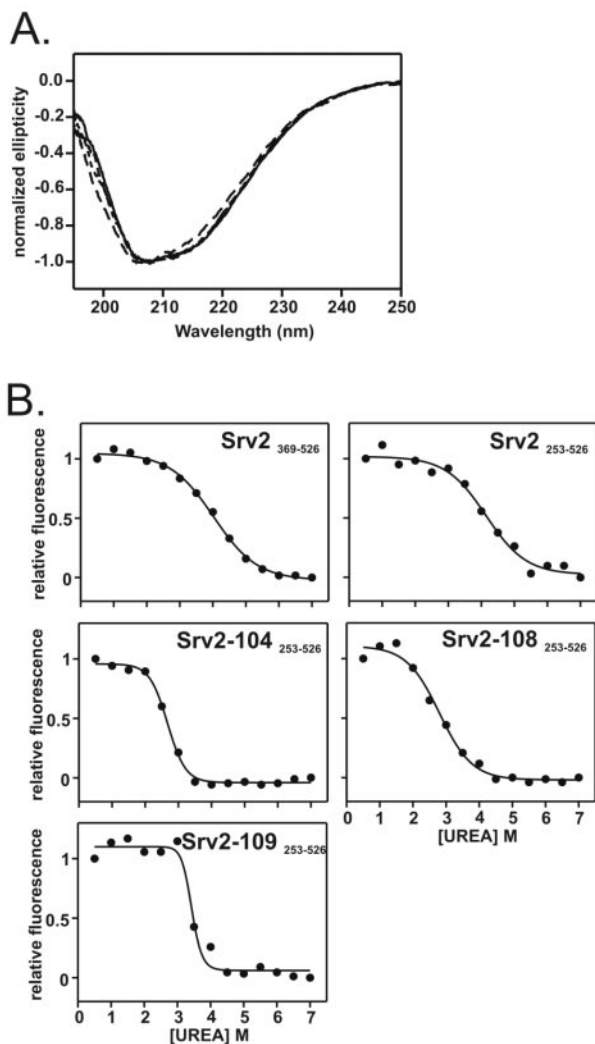
A.

B.

Figure 9. Structure and stability of wild-type and mutant Srv2 proteins. (A) The folding of wild-type and mutant Srv2$_{253-526}$ proteins was compared by measuring the far UV CD spectra. The spectra of wild-type Srv2$_{253-526}$ (solid line), Srv2-104$_{253-526}$ (dashed line, "longest dashes"), Srv2-108$_{253-526}$ (dashed line, "medium dashes"), and Srv2-109$_{253-526}$ (dashed line, "shortest dashes") are almost identical, suggesting similar structures. (B) The stability of wild-type Srv2$_{253-526}$ and Srv2$_{369-526}$ proteins, and mutant Srv2$_{253-526}$ proteins defective in actin binding, were measured by fluorescence-monitored urea denaturation assay. The normalized fluorescence is shown on the *y*-axis and the urea concentration on the *x*-axis. Both wild-type Srv2 fragments unfold at ~4 M urea. The mutants unfold at a slightly lower urea concentration, 2.5–3.5 M.

lack detectable actin-binding affinity. From these analyses, it is still unclear how the adjacent sequences contribute to high-affinity ADP-actin binding without showing any actin binding on their own. We considered that they might alter the oligomerization state of the C-terminus, thereby strengthening actin-binding affinity indirectly. However, analytical gel filtration analysis showed that both the shorter (369–526) and longer (253–526) Srv2 fragments dimerize (Quintero-Monzon and Goode, unpublished data). This leaves at least two open possibilities. First, the 253–373 sequence may in fact bind directly to actin, but only in the structural context of the β-sheet region (i.e., they fold together to form a high-affinity actin-binding site). Second, the β-sheet may bind to actin first, altering its conformation to expose a cryptic second actin-binding site within the 253–373 sequence. In either case, future mutational analyses in this region should help define how these sequences contribute to strong actin-binding affinity.

Our data also implicate specific subdomains of actin in binding Srv2/CAP. The ability of Srv2 to compete directly with cofilin for binding ADP-actin monomers suggests that they have at least partially overlapping binding sites on actin. Consistent with this idea, the binding sites for Srv2/CAP and cofilin are suggested to reside in subdomains 1 and 3 of actin (Rodal *et al.*, 1999; Rommelaere *et al.*, 2003). Also in support of this view, we have found that mutations in this region of actin are suppressed by overexpression of Srv2 in vivo (Hendries and Goode, unpublished observations). However, although the Srv2-actin and cofilin-actin interactions may be overlapping, they must also be unique, which is supported by two observations. First, cofilin strongly inhibits nucleotide exchange on actin monomers, whereas Srv2/CAP does not (Moriyama and Yahara, 2002; Balcer *et al.*, 2003). Second, cofilin-bound actin monomers are free to assemble onto barbed ends of actin filaments, whereas Srv2-bound actin monomers are blocked (Figure 4). Thus, Srv2/CAP and cofilin must make distinct contacts on actin. It is likely that Srv2/CAP makes specific contacts at the pointed end of the actin monomer (subdomains II and IV), similar to thymosins (Hertzog *et al.*, 2004), to explain its inhibition of barbed end growth. However, the WH2 domain of Srv2 is not required for these interactions, because Srv2$_{369-526}$, which lacks the WH2 domain, also inhibits barbed end growth (Figure 4E).

One unexpected result in our study was the lack of a significant contribution made to actin binding by the WH2 domain of Srv2/CAP. WH2 domains are signature actin-binding motifs that show a strong preference for binding ATP-actin monomers (Paunola *et al.*, 2002). Further, all CAP family members, spanning the animal, plant, and fungal kingdoms, contain a WH2 domain at this position in the C-terminus (Figure 1A), suggesting that this element is important for function. However, our mutation at the residues that in other WH2 domains are critical for actin-binding caused no significant effect on the ADP-actin binding affinity, only a minor change in ATP-actin binding affinity, and no detectable effect on Srv2/CAP function in vivo. Thus, it remains unclear what function is served by the WH2 domain in Srv2/CAP, other than modestly facilitating ATP-G-actin binding. One possibility is that in Srv2/CAP proteins this domain has additional structural roles. It is interesting to note that CAP family members all contain a small insertion of 3–4 residues located near the key actin-binding site at the N-terminal α-helix in WH2 domains (Hertzog *et al.*, 2004). This insertion is not found in other WH2 domain-containing proteins (see Paunola *et al.*, 2002) and therefore, could tailor the WH2 domain for CAP-specific functions, including possibly a structural role.

Our data also lend important insights into the molecular arrangement of the Srv2/CAP complex. A number of previous studies have shown that Srv2/CAP exists in a HMW complex in cell extracts and that purified Srv2/CAP proteins oligomerize via interactions within and between their N- and C-termini. More recently, native Srv2 complex (~600 kDa) was isolated from *S. cerevisiae* and found to be comprised of only two proteins, actin and Srv2, present in a 1:1 M ratio (Balcer *et al.*, 2003). It was suggested that the complex contains six actin monomers and six Srv2 molecules. How these 12 molecules are organized into a macromolec-
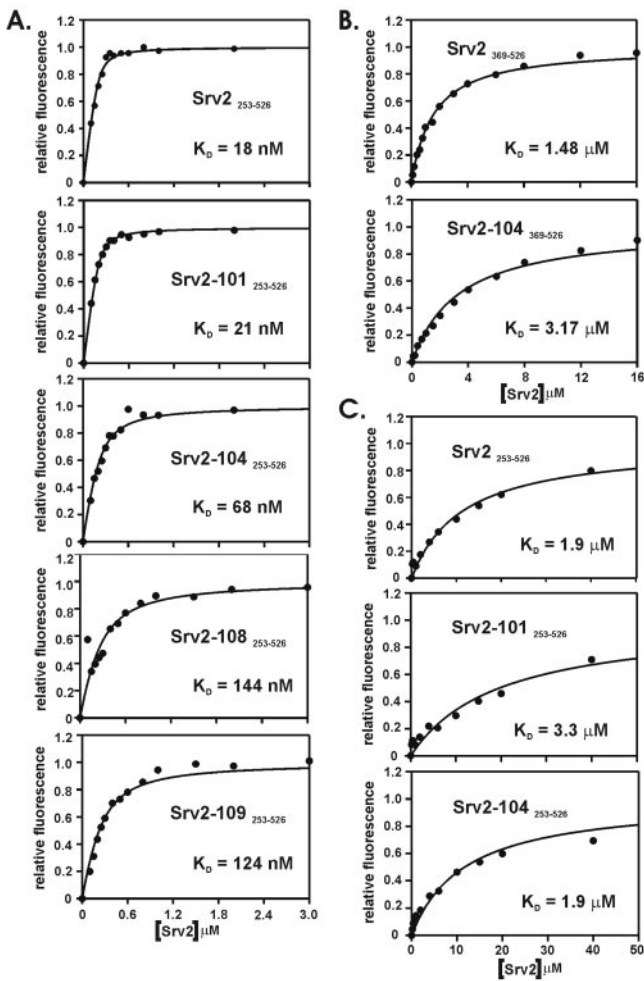
Figure 10. Srv2 alleles that show defects in vivo weaken binding of Srv2 to ADP-actin in vitro. (A) The same assay as described in Figure 2 was used to measure binding affinities of mutant Srv2 fragments for ADP-G-actin. (B) The Srv2-104 mutation impairs binding to ADP-G-actin in Srv2-104$_{369-526}$. (C) The same assay as in Figure 3A was used to measure the binding affinities of Srv2$_{253-526}$ mutants for ATP-G-actin. All data are summarized in Table 3.

ular complex (involving intra- and intermolecular interactions between Srv2 domains and between Srv2 and G-actin) presents a challenging puzzle. We note that in the crystallized C-terminal β-sheet (see Figure 6), the two Srv2 molecules face in opposite directions with 180° symmetry. We have defined three well-separated surfaces on this structure that are important for ADP-actin binding (disrupted by *srv2-104*, *srv2-108*, and *srv2-109*). Interestingly, the residues mutated in each of these sites (E385, D461, K462, K472, E473) point in the same direction on one Srv2 molecule in the dimer, raising the possibility that only one face of the structure mediates actin binding. This predicted actin-binding face corresponds to the "back" side of the Srv2 molecule on the left in Figure 6 (colored in yellow) and the "front" side of the Srv2 molecule on the right (colored in aqua). These data provide a conceptual framework for future studies aimed at modeling the Srv2/CAP-actin interaction at higher resolution and orienting these interactions within the HMW complex.

Srv2/CAP Mechanism and Cellular Function

As discussed above, a key cellular function of Srv2/CAP is to promote cofilin-dependent actin turnover. The mechanism is proposed to involve Srv2/CAP competing with cofilin for binding to ADP-actin monomers, thus recycling cofilin for new rounds of filament disassembly. This mechanism requires that Srv2/CAP be able to bind with high affinity to ADP-actin, which we have demonstrated here. Previous studies have shown that cofilins bind ADP-actin monomers with high affinity (K_d = 0.02–0.1 μM) (Carlier *et al.*, 1997; Blanchoin and Pollard, 1998; Vartiainen *et al.*, 2002). Our data show that Srv2$_{253-269}$ fragment binds to ADP-actin at least as strongly as cofilin. Additional contributions to this competition mechanism may come from the N-terminus of Srv2/CAP, which associates directly with cofilin in vitro (Moriyama and Yahara, 2002). One exciting possibility is that binding of the N-terminus of CAP to cofilin might weaken cofilin's affinity for ADP-actin. Thus, the N- and C-termini of Srv2/CAP may work together to rapidly displace cofilin from ADP-actin monomers. Consistent with this idea, intact yeast Srv2 complex converts cofilin-bound ADP-actin monomers to ATP-actin at below 1:100 M stoichiometries, suggesting a catalytic activity (Balcer *et al.*, 2003). Importantly, we have demonstrated that the high-affinity Srv2-ADP-actin interaction is required for its cellular function, because there is a close correlation between the in vitro defects in actin binding for *srv2-104*, *srv2-108*, and *srv2-109* and the defects they cause in actin organization and cell morphology in vivo.

In the next step of the mechanism, Srv2-bound ADP-actin monomers undergo rapid exchange of nucleotide (ATP for ADP; Moriyama and Yahara, 2002; Balcer *et al.*, 2003). We propose that there is a subsequent "handoff" of ATP-actin monomers from Srv2/CAP to other actin monomer binding proteins such as profilin, which facilitate barbed end actin polymerization. This step is necessary, because Srv2/CAP-bound actin monomers are blocked from associating with barbed ends of filaments. Further, the Srv2/CAP complex is tethered to actin filaments through its interactions with Abp1 and thus is not available to chaperone actin monomers to filament ends. It remains to be determined exactly how the proposed handoff works, but our data offer a feasible model. We show that Srv2/CAP has relatively weak affinity for ATP-actin monomers, which is consistent with Srv2/CAP releasing actin after nucleotide exchange has occurred, presumably to be bound by proteins with higher affinity for ATP-actin monomers, such as profilin or WASp (Vinson *et al.*, 1998; Marchand *et al.*, 2000). Consistent with this possibility, we find that profilin partially relieves the inhibition of barbed end assembly by CAP (Figure 4). Profilin and Srv2 also are reported to physically interact (Drees *et al.*, 2000), which might further facilitate a monomer handoff. These events would lead to regeneration of the ATP-actin monomer pool available for new rounds of polymerization and prime Srv2/CAP for subsequent rounds of recycling cofilin and actin.

REFERENCES

Amatruda, J.F., and Cooper, J.A. (1992). Purification, characterization, and immunofluorescence localization of *Saccharomyces cerevisiae* capping protein. J. Cell Biol. *117*, 1067–1076.

Balcer, H.I., Goodman, A.L., Rodal, A.A., Smith, E., Kugler, J., Heuser, J.E., and Goode, B.L. (2003). Coordinated regulation of actin filament turnover by a high-molecular-weight Srv2/CAP complex, cofilin, profilin, and Aip1. Curr. Biol. *13*, 2159–2169.

Barrero, R.A., Umeda, M., Yamamura, S., and Uchimiya, H. (2002). *Arabidopsis* CAP regulates the actin cytoskeleton necessary for plant cell elongation and division. Plant Cell *14*, 149–163.

Baum, B., Li, W., and Perrimon, N. (2000). A cyclase-associated protein regulates actin and cell polarity during *Drosophila* oogenesis and in yeast. Curr. Biol. *10*, 964–973.

Benlali, A., Draskovic, I., Hazelett, D.J., and Treisman, J.E. (2000). *act up* controls actin polymerization to alter cell shape and restrict Hedgehog signaling in the *Drosophila* eye disc. Cell *101*, 271–281.

Bertling, E., Hotulainen, P., Mattila, P.K., Matilainen, T., Salminen, M., and Lappalainen, P. (2004). Cyclase-associated protein 1 (CAP1) promotes cofilin-induced actin dynamics in mammalian nonmuscle Cells. Mol. Biol. Cell *15*, 2324–2334.

Blanchoin, L., and Pollard, T.D. (1998). Interaction of actin monomers with *Acanthamoeba actophorin* (ADF/cofilin) and profilin. J. Biol. Chem. *273*, 25106–25111.

Carlier, M.F., Jean, C., Rieger, K.J., Lenfant, M., and Pantaloni, D. (1993). Modulation of the interaction between G-actin and thymosin β_4 by the ATP/ADP ratio: possible implication in the regulation of actin dynamics. Proc. Natl. Acad. Sci. USA *90*, 5034–5038.

Carlier, M.F., Laurent, V., Santolini, J., Melki, R., Didry, D., Xia, G.X., Hong, Y., Chua, N.H., and Pantaloni, D. (1997). Actin depolymerizing factor (ADF/cofilin) enhances the rate of filament turnover: implication in actin-based motility. J. Cell Biol. *136*, 1307–1322.

Detmers, P., Weber, A., Elzinga, M., and Stephens, R.E. (1981). 7-Chloro-4-nitrobenzeno-2-oxa-1,3-diazole actin as a probe for actin polymerization. J. Biol. Chem. *256*, 99–105.

Dewar, H., Warren, D.T., Gardiner, F.C., Gourlay, C.G., Satish, N., Richardson, M.R., Andrews, P.D., and Ayscough, K.R. (2002). Novel proteins linking the actin cytoskeleton to the endocytic machinery in *Saccharomyces cerevisiae.* Mol. Biol. Cell *13*, 3646–3661.

Dodatko, T. *et al.* (2005). Crystal structure of the actin binding domain of the cyclase-associated protein. Biochemistry *43*, 10628–10641.

Drees, B.L. *et al.* (2001). A protein interaction map for cell polarity development. J. Cell Biol. *154*, 549–571.

Fedor-Chaiken, M., Deschenes, R.J., and Broach, J.R. (1990). *SRV2*, a gene required for *RAS* activation of adenylate cyclase in yeast. Cell *61*, 329–340.

Field, J. *et al.* (1990). Cloning and characterization of *CAP*, the *S. cerevisiae* gene encoding the 70 kd adenylyl cyclase-associated protein. Cell *61*, 319–327.

Freeman, N.L., Chen, Z., Horenstein, J., Weber, A., and Field, J. (1995). An actin monomer binding activity localizes to the carboxyl-terminal half of the *Saccharomyces cerevisiae* cyclase-associated protein. J. Biol. Chem. *270*, 5680–5685.

Freeman, N.L., Lila, T., Mintzer, K.A., Chen, Z., Pah, A.J., Ren, R., Drubin, D.G., and Field, J. (1996). A conserved proline-rich region of *Saccharomyces cerevisiae* cyclase-associated protein binds SH3 domains and modulates cytoskeletal localization. Mol. Cell. Biol. *16*, 548–556.

Gerst, J.E., Ferguson, K., Vojtek, A., Wigler, M., and Field, J. (1991). CAP is a bifunctional component of the *Saccharomyces cerevisiae* adenylyl cyclase complex. Mol. Cell. Biol. *11*, 1248–1257.

Gieselmann, R., and Mann, K. (1992). ASP-56, a new actin sequestering protein from pig platelets with homology to CAP, an adenylate cyclase-associated protein from yeast. FEBS Lett. *298*, 149–153.

Gottwald, U., Brokamp, R., Karakesisoglou, I., Schleicher, M., and Noegel, A.A. (1996). Identification of a cyclase-associated protein (CAP) homologue in *Dictyostelium discoideum* and characterization of its interaction with actin. Mol. Biol. Cell *7*, 261–272.

Hertzog, M., Yarmola, E.G., Didry, D., Bubb, M.R., and Carlier, M.-F. (2002). Control of actin dynamics by proteins made of β-thymosin repeats: the actobindin family. J. Biol. Chem. *277*, 14786–14792.

Hertzog, M. *et al.* (2004). The β-thymosin/WH2 domain: structural basis for the switch from inhibition to promotion of actin assembly. Cell *117*, 611–623.

Hubberstey, A., Yu, G., Loewith, R., Lakusta, C., and Young, D. (1996). Mammalian CAP interacts with CAP, CAP2, and actin. J. Cell Biochem. *61*, 459–466.

Hubberstey, A.V., and Mottillo, E.P. (2002). Cyclase-associated proteins: CA-Pacity for linking signal transduction and actin polymerization. FASEB J. *16*, 487–499.

Ksiazek, D. *et al.* (2003). Structure of the N-terminal domain of the adenylyl cyclase-associated protein (CAP) from *Dictyostelium discoideum.* Structure *11*, 1171–1178.

Lappalainen, P., Fedorov, E.V., Fedorov, A.A., Almo, S.C., and Drubin, D.G. (1997). Essential functions and actin-binding surfaces of yeast cofilin revealed by systematic mutagenesis. EMBO J. *16*, 5520–5530.

Lila, T., and Drubin, D.G. (1997). Evidence for physical and functional interactions among two *Saccharomyces cerevisiae* SHB domain proteins, an adenylyl cyclase-associated protein and the actin cytoskeleton. Mol. Biol. Cell *8*, 367–385.

Maciver, S.K., and Weeds, A.G. (1994). Actophorin preferentially binds monomeric ADP-actin over ATP-bound actin: consequences for cell locomotion. FEBS Lett. *347*, 251–256.

Marchand, J.B., Kaiser, D.A., Pollard, T.D., and Higgs, H.N. (2000). Interaction of WASP/Scar proteins with actin and vertebrate Arp2/3 complex. Nat. Cell Biol. *3*, 76–82.

Mattila, P.K., Salminen, M., Yamashiro, T., and Lappalainen, P. (2003). Mouse MIM, a tissue-specific regulator of cytoskeletal dynamics, interacts with ATP-actin monomers through its C-terminal WH2 domain. J. Biol. Chem. *278*, 8452–8459.

Moriyama, K., and Yahara, I. (2002). Human CAP1 is a key factor in the recycling of cofilin and actin for rapid actin turnover. J. Cell Sci. *115*, 1591–1601.

Moseley, J.B., Sagot, I., Manning, A.L., Xu, Y., Eck, M.J., Pellman, D., and Goode, B.L. (2003). A conserved mechanism for Bni1- and mDia1-induced actin assembly and dual regulation of Bni1 by Bud6 and profilin. Mol. Biol. Cell *15*, 896–907.

Noegel, A.A., Blau-Wasser, R., Sultana, H., Muller, R., Israel, L., Schleicher, M., Patel, H., and Weijer, C.J. (2004). The cyclase-associated protein CAP as regulator of cell polarity and cAMP signaling in *Dictyostelium.* Mol. Biol. Cell *15*, 934–945.

Ojala, P.J., Paavilainen, V.O., Vartiainen, M.K., Tuma, R., Weeds, A.G., and Lappalainen, P. (2002). The two ADF-H domains of twinfilin play functionally distinct roles in interactions with actin monomers. Mol. Biol. Cell *13*, 3811–3821.

Pardee, J.D., and Spudich, J.A. (1982). Purification of muscle actin. Methods Cell Biol. *24*, 271–289.

Paunola, E., Mattila, P.K., and Lappalainen, P. (2002). WH2 domain: a small, versatile adapter for actin monomers. FEBS Lett. *513*, 92–97.

Peränen, J., Rikkönen, M., Hyvonen, M., and Kääriäinen, L. (1996). T7 vectors with modified T7*lac* promoter for expression of proteins in *Escherichia coli.* Anal. Biochem. *236*, 371–373.

Pollard, T.D. (1986). Rate constants for the reactions of ATP- and ADP-actin with the ends of actin filaments. J. Cell Biol. *103*, 2747–2754.

Rodal, A.A., Tetreault, J.W., Lappalainen, P., Drubin, D.G., and Amberg, D.C. (1999). Aip1p interacts with cofilin to disassemble actin filaments. J. Cell Biol. *145*, 1251–1264.

Rommelaere, H., Waterschoot, D., Neirynck, K., Vandekerckhove, J., and Ampe, C. (2003). Structural plasticity of functional actin: pictures of actin binding protein and polymer interfaces. Structure *11*, 1279–1289.

Rose, M.D., Winston, F., and Hieter, P. (1989). Methods in Yeast Genetics, Cold Spring Harbor, NY: Cold Spring Harbor Laboratory Press, 198 pp.

Sikorski, R.S., and Hieter, P. (1989). A system of shuttle vectors and yeast host strains designed for efficient manipulation of DNA in *Saccharomyces cerevisiae.* Genetics *122*, 19–27.

Vaduva, G., Martinez-Quiles, N., Anton, I.M., Martin, N.C., Geha, R.S., Hopper, A.K., and Ramesh, N. (1999). The human WASp-interacting protein, WIP, activates the cell polarity pathway in yeast. J. Biol. Chem. *274*, 17103–17108.

Van Troys, M., Dewitte, D., Goethals, M., Carlier, M.F., Vandekerckhove, J., and Ampe, C. (1996). The actin binding site of thymosin β_4 mapped by mutational analysis. EMBO J. *15*, 201–210.

Vartiainen, M.K., Mustonen, T., Mattila, P.K., Ojala, P.J., Thesleff, I., Partanen, J., and Lappalainen, P. (2002). The three mouse actin-depolymerizing factor/cofilins evolved to fulfill cell-type-specific requirements for actin dynamics. Mol. Biol. Cell *13*, 183–194.

Vinson, V.K., De La Cruz, E.M., Higgs, H.N., and Pollard, T.D. (1998). Interactions of *Acanthamoeba* profilin with actin and nucleotides bound to actin. Biochemistry *37*, 10871–10880.

Vojtek, A., Haarer, B., Field, J., Gerst, J., Pollard, T.D., Brown, S., and Wigler, M. (1991). Evidence for a functional link between profilin and CAP in the yeast *S. cerevisiae.* Cell *66*, 497–505.

Weeds, A.G., Harris, H., Gratzer, W., and Gooch, J. (1986). Interactions of pig plasma gelsolin with G-actin. Eur. J. Biochem. *161*, 77–84.

Wolven, A.K., Belmont, L.D., Mahoney, N.M., Almo, S.C., and Drubin, D.G. (2000). In vivo importance of actin nucleotide exchange catalyzed by profilin. J. Cell Biol. *150*, 895–904.

Yamaguchi, H., Miki, H., Suetsugu, S., Ma, L., Kirschner, M.W., and Takenawa, T. (2000). Two tandem verprolin homology domains are necessary for a strong activation of Arp2/3 complex-induced actin polymerization and induction of microspike formation by N-WASp. Proc. Natl. Acad. Sci. USA *97*, 12631–12636.

Yu, J., Wang, C., Palmieri, S.J., Haarer, B.K., and Field, J. (1999). A cytoskeletal localizing domain in the cyclase-associated protein, CAP/Srv2p, regulates access to a distant SH3-binding site. J. Biol. Chem. *274*, 19985–19991.

Zelicof, A., Protopopov, V., David, D., Lin, X.Y., Lustgarten, V., and Gerst, J.E. (1996). Two separate functions are encoded by the carboxyl-terminal domains of the yeast cyclase-associated protein and its mammalian homologs. Dimerization and actin binding. J. Biol. Chem. *271*, 18243–18252.